JACS
JOURNAL OF THE AMERICAN CHEMICAL SOCIETY
Article
pubs.acs.org/JACS

Evidence for Metal−Surface Interactions and Their Role in Stabilizing Well-Defined Immobilized Ru−NHC Alkene Metathesis Catalysts

Manoja K. Samantaray,[†] Johan Alauzun,[‡] David Gajan,[§] Santosh Kavitake,[†] Ahmad Mehdi,[‡] Laurent Veyre,[†] Moreno Lelli,[∥] Anne Lesage,[∥] Lyndon Emsley,[∥] Christophe Copéret,[§,*] and Chloé Thieuleux*[,†]

[†]C2P2, UMR 5265, Université de Lyon, Institut de Chimie de Lyon, UMR 5265 CNRS-Université Lyon 1-ESCPE Lyon, LC2P2, Equipe COMS, ESCPE Lyon, 69616 Villeurbanne, France

[‡]Institut Charles Gerhardt UMR 5352, Chimie Moléculaire et Organisation du Solide, Université Montpellier 2, 34095 Montpellier Cedex 5, France

[§]Department of Chemistry, ETH Zürich, CH-8093 Zürich, Switzerland

[∥]Centre de RMN à Très Hauts Champs, Université de Lyon (CNRS/ENS Lyon/UCB Lyon 1), 69100 Villeurbanne, France

Supporting Information

ABSTRACT: Secondary interactions are demonstrated to direct the stability of well-defined Ru−NHC-based heterogeneous alkene metathesis catalysts. By providing key stabilization of the active sites, higher catalytic performance is achieved. Specifically, they can be described as interactions between the metal center (active site) and the surface functionality of the support, and they have been detected by surface-enhanced $^{1}H-^{29}Si$ NMR spectroscopy of the ligand and ^{31}P solid-state NMR of the catalyst precursor. They are present only when the metal center is attached to the surface via a flexible linker (a propyl group), which allows the active site to either react with the substrate or relax, reversibly, to the surface, thus providing stability. In contrast, the use of a rigid linker (here mesitylphenyl) leads to a well-defined active site far away from the surface, stabilized only by a phosphine ligand which under reaction conditions leaves probably irreversibly, leading to faster decomposition and deactivation of the catalysts.

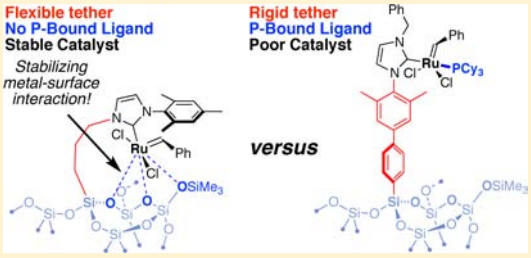

INTRODUCTION

Ruthenium-catalyzed alkene metathesis has a profound impact on a wide range of applications, from performance polymers to complex natural products and promising pharmaceutical leads.[1] Substantial research efforts to improve the performance of ruthenium alkene metathesis catalysts have been undertaken in recent years.[2] In particular, a considerable amount of work has focused on obtaining corresponding heterogeneous catalysts with the aim to improve the efficiency of processes, including the simplified removal of Ru contaminants.[3]

In this context, we have recently developed tailored functional mesostructured materials containing regularly distributed Ru−N-heterocyclic carbene (NHC) moieties.[4] The controlled incorporation of the precursor ligand in the silica matrix[5] and the subsequent surface grafting of Ru complexes[6] yielded well-defined, active, and reusable catalytic sites. Although we have shown that these Ru−NHC complexes were highly efficient in the self-metathesis of ethyl oleate, with performances close to those obtained for equivalent homogeneous analogues,[4] we had little understanding on the nature of the active sites and in particular what the role of the surface functionalities was in affecting the activity and the stability of the electron deficient Ru catalytic sites.

Here, we show that supported Ru−NHC alkene metathesis catalysts (Scheme 1) are significantly more stable and display higher catalytic performances when they are bound to the surface with a flexible tether. Detailed solid-state NMR investigations on both the precursors and on the catalysts suggest that this results from the interaction between the active metal center and surface functionalities.

Ru−NHC catalysts were prepared via sol−gel strategies based on supramolecular interactions between the silica precursor, the functional silane precursor, and the structure-directing agent to secure the regular localization of the organic functionalities along the pore channels of the mesostructured silica matrix,[4,5b,7] which were then transformed into supported NHC−metal complexes. Two classes of catalysts were investigated having either (i) a flexible alkyl tether (**Mat-RuF**) to promote interactions between the metal center (the active site) and the silica surface (support), here a propyl, or (ii) a rigid aromatic tether (**Mat-RuR**) to prevent such interactions, here a mesitylphenyl (Scheme 1). The ligand−surface interactions were characterized at an atomic level on the precursors by dynamic nuclear polarization surface-enhanced

Received: November 30, 2012
Published: January 30, 2013

   dx.doi.org/10.1021/ja311722k | J. Am. Chem. Soc. 2013, 135, 3193−3199

Scheme 1. (a) Synthesis of NHC−Ru Alkene Metathesis Catalysts from the Corresponding Imidazolium Derivatives[a] and Structures for (b) Mat-RuF, (c) Mat-RuR, and (d,e) the Corresponding Homogeneous Catalysts[b]

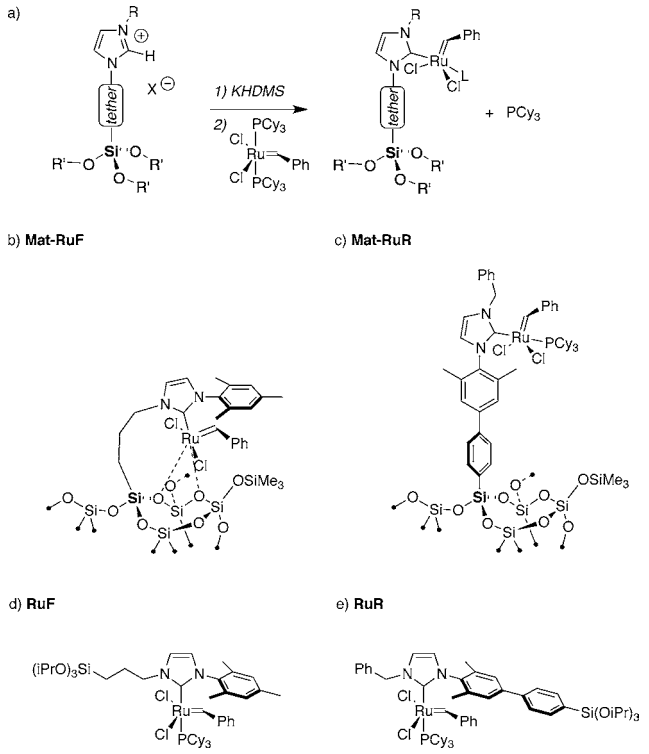

[a]R = Ms or CH_2Ph, tether = Pr (F) or PhMs (R), OR′ = OiPr or O of the silica surface, and L = PCy_3 or silica surface. [b]The silica surface being amorphous, the structure of the surface species is to be taken as a representative example based on available data (see text).

NMR spectroscopy (DNP SENS)[8] and were shown to influence the structure of the resulting Ru−NHC surface species, supported by ^{31}P NMR results, as well as their catalytic performances.

RESULTS AND DISCUSSIONS

The imidazolium materials were prepared using a sol−gel process in the presence of a structure-directing agent (here P123, a block copolymer). The targeted material was obtained by co-hydrolysis and co-condensation of an organotrialkoxysilane precursor with tetraethoxysilane as a diluent. A dilution of 1/30 has been chosen to ensure that the distance between organic functionality is ca. 1 nm. For the flexible tether, the material was prepared from iodopropyltriethoxysilane. The corresponding iodopropyl material was postreacted with mesitylimidazole to give the imidazolium-containing material (**Mat-ImF**) as previously reported.[4] All these materials are highly mesoporous with a narrow pore size distribution centered at ca. 7 nm according to N_2 adsorption/desorption measurement (calculated by the BJH method using the adsorption branch of the N_2 adsorption isotherm). Transmission electron microscopy and small-angle X-ray diffraction are consistent with the formation of a 2D hexagonal arrangement of the porous network (see Supporting Information). The material with the rigid tether (**Mat-ImR**), having similar textural characteristics (pore size, ca. 580 m^2/g and pore volume, ca. 0.8 cm^3/g) to **Mat-ImF**, was prepared

Scheme 2. Synthesis of Mat-RuR

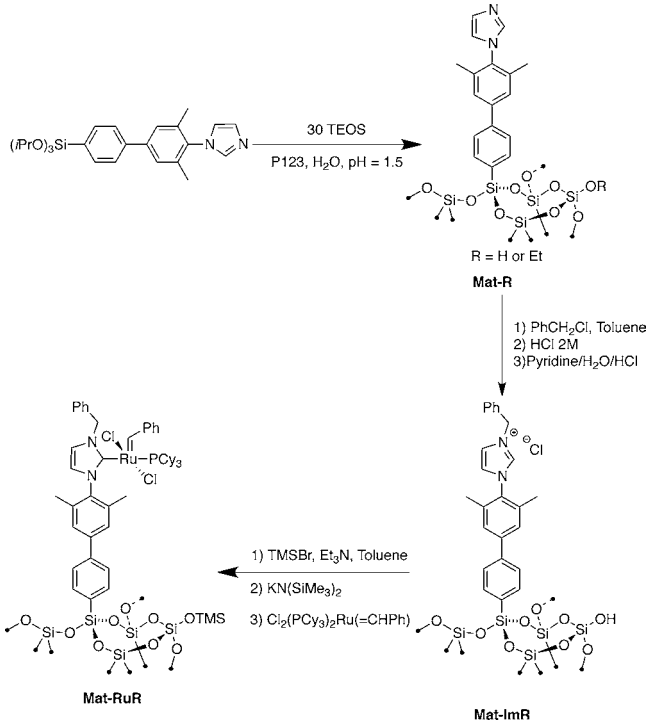

from a molecular precursor having an imidazole terminal group, which was further transformed into an imidazolium by post-reaction with benzyl chloride yielding **Mat-ImR** (Scheme 2; see Supporting Information for details).

Detailed characterization by solid-state NMR spectroscopy of these materials was then performed, in particular to understand the ligand orientation with respect to the surface. Two-dimensional $^1H-^{29}Si$ (Figure 1) were recorded at natural isotopic abundance by using DNP SENS, a recently introduced technique that has been shown to provide surface signal enhancements of up to a factor ∼100 with respect to conventional NMR instrumentation.[8] In DNP SENS, a paramagnetic polarizing agent is introduced by incipient wetness impregnation of the material with a radical containing solution in a suitable solvent. Microwave irradiation of the EPR transition at low temperature (∼100 K) yields ^1H DNP enhancements of the frozen solid. Cross-polarization can then be used to transfer the enhanced ^1H magnetization selectively to the heteronuclei present on the material surface.

NMR samples of **Mat-ImR** or **Mat-ImF** were prepared by impregnation with a 12 mM aqueous solution of TOTAPOL.[9] Cross-polarization magic angle spinning (CP-MAS) NMR spectra were acquired at 9.4 T (400 MHz ^1H Larmor frequency), using a commercial Bruker 400 MHz/263 GHz gyrotron DNP system (see the Supporting Information for details). The resulting two-dimensional $^1H-^{29}Si$ correlation NMR spectra of **Mat-ImR** and **Mat-ImF** are shown in Figure 1. The short mixing time (400 μs) used in the CP step ensures correlations are observed only between spins in close spatial proximity to one another. As expected, in both materials we see correlations between the silicon *T*-sites and the nearest protons (aromatic protons for **Mat-ImR** and aliphatic protons for **Mat-ImF**; the weaker intensity of the T_3cross-peak in **Mat-ImR** compared to the T_3 cross-peak in **Mat-ImF** is accounted for by the longer distance between ^1H and T_3-Si spins in **Mat-ImR**). In water the SiOH protons are expected to correlate with the Q

dx.doi.org/10.1021/ja311722k | J. Am. Chem. Soc. 2013, 135, 3193−3199

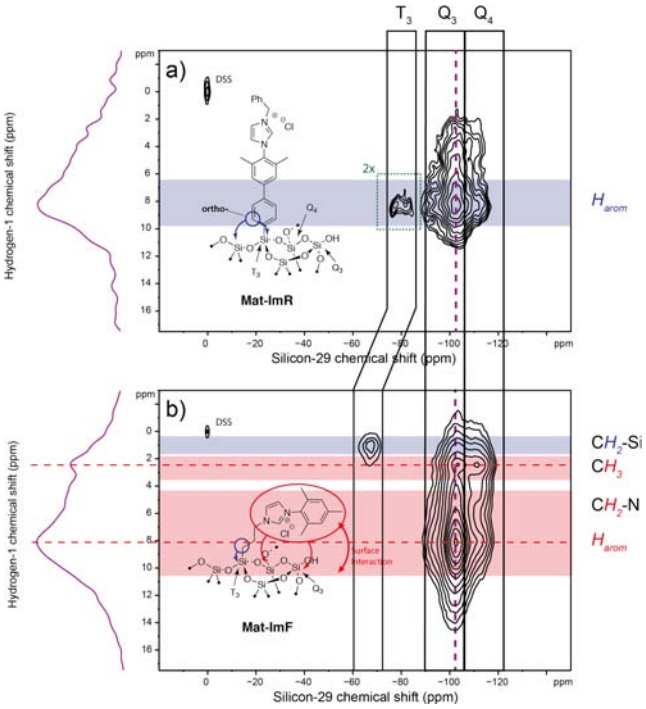

Figure 1. Contour plots of two-dimensional 9.4 T ^{1}H−^{29}Si HETCOR DNP SENS spectra for the materials **Mat-ImR** (a) and **Mat-ImF** (b). The blue bands show the expected correlations among the surface T_n sites and the ortho protons (a) and the CH_2−Si protons (b) of the ligands. In panel b, the red bands show the expected positions for correlations between the surface Q_n silicon atoms and the methyl and aromatic protons of the ligand. These correlations indicate that the flexible linker in **Mat-ImF** is folded to allow interaction with the surface. To the left of each spectrum the traces perpendicular to the silicon axes, taken at the silicon frequency indicated by the violet dashed lines, are shown. Similar conditions were used to acquire both spectra (full experimental details are given in the Supporting Information). The DNP enhancements were ε_H = 30 and 26 for the spectra acquired on **Mat-ImR** (a) and **Mat-ImF** (b), respectively. A minute amount of sodium 2,2-dimethyl-2-silapentane-5-sulfonate (DSS), added to the water solution prior to impregnation of the materials, was used as internal standard to calibrate ^{1}H and ^{29}Si chemical shifts. A green box in panel a reports the T_n sites with a 2-fold increased intensity.

sites at around 4 ppm and to give a broad peak superimposed with the other proton resonances of **Mat-ImR** and **Mat-ImF**. Also as expected, in the material with the rigid tether (**Mat-ImR**) we observe correlations between surface Q_n sites and the aromatic protons of the tether. The key finding in these spectra is that clear correlations are observed between Q_n sites and the aromatic and methyl resonances from the imidazolium and mesityl fragments in the ^{1}H−^{29}Si correlation spectrum of **Mat-ImF** (Figure 1b). This spectrum shows that the flexible tether allows the phenyl ring and the attached methyl groups to fold back onto the surface. Conversely, the absence of correlations between the methyl resonance of the mesityl ligand and the surface resonances in **Mat-ImR** indicates that such ligand−surface interactions are nonexistent in this material and that this groups lies away from the surface. The observation for the **Mat-ImF** is counterintuitive since, in water, the positively charged imidazolium ring should prompt the tether to orient away from the surface, and suggests that this interaction is unexpectedly strong. The interactions are also observed when tetrachloroethane is used as the impregnating solvent for DNP-SENS (Figure S14).

Mat-ImR and **Mat-ImF** were converted into the target Ru−NHC-containing catalytic materials in a two-step sequence: (i) passivation of the surface silanols by trimethylsilyl groups and (ii) grafting of $[(Cl)_2Ru(=CHPh)(PCy_3)_2]$ using K{N-$(SiMe_3)_2$} (2 equiv/imidazolium) as a base (Scheme 1a). The Ru loading obtained from elemental analysis (ca. 1.4%$_{wt}$) shows the presence of ca. 0.3 Ru per organic functionality for both systems as typically observed when grafting metal complexes on imidazolium-containing materials is performed with K{N-$(SiMe_3)_2$}.[4,7] A detailed ^{1}H, ^{13}C and ^{29}Si NMR characterization could not be performed on the catalysts, since so far the DNP approach provided no signal enhancement in these materials (probably because of the interaction/reaction of the polarizing radical and the Ru center). Key structural features were nevertheless determined from ^{31}P MAS solid-state NMR spectroscopy. For **Mat-RuF** only one signal at 47 ppm is observed, characteristic of P(V) products (Figure 2a,

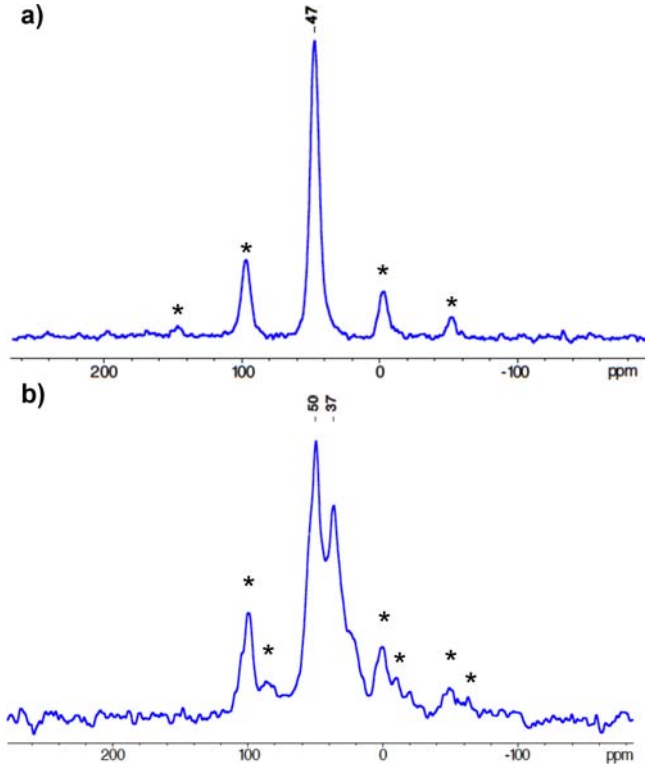

Figure 2. ^{31}P CPMAS solid-state NMR spectra of (a) **Mat-RuF** (3584 scans, recycle delay = 2 s and contact time = 2 ms) and of (b) **Mat-RuR** (3000 scans, recycle delay = 2 s and contact time = 2 ms); the peaks at 50 and 37 ppm are in ca. 2:1 ratio (under CP-MAS conditions, intensities are not quantitative, and ratio only indicative). All * indicate spinning side bands (MAS frequency = 10 kHz).

phosphorus-31 NMR), that result from the reaction of free PCy_3 with the silica surface.[11] Note the absence of a phosphorus signal associated with coordination of PCy_3 to Ru, expected at 36 ppm. This result indicates that the two PCy_3 ligands, previously present in $[(Cl)_2Ru(=CHPh)(PCy_3)_2]$ are liberated during grafting and undergo reaction with the surface; it also implies that the NHC−Ru center attached to the surface with a flexible tether has no phosphine bound and interacts with the oxygen of the surface of the material, presumably an $OSiMe_3$ group or a siloxane bridge,[12] to stabilize the otherwise

dx.doi.org/10.1021/ja311722k | J. Am. Chem. Soc. 2013, 135, 3193−3199

unstable 14- electron species (Scheme 1b). In contrast, the phosphorus-31 CP MAS solid-state NMR spectrum of **Mat-RuR** contains two signals of similar intensity for both the P(V) product and PCy_3 coordinated to Ru (Figure 2b). With the rigid tether, only one free PCy_3 ligand is generated, the other remains coordinated to the Ru center since the rigid tether prevents stabilization by the surface functionalities (Scheme 1c). Although it was not possible to obtain a direct evidence for the structure of the alkylidene species via SENS NMR, as was described for the precursor, the observed absence of interactions of the imidazolium moiety with the silica surface in **Mat-ImR** combined with the presence of PCy_3 coordinated to Ru in **Mat-RuR** strongly suggests the formation of a NHC−Ru alkylidene complex coordinated to PCy_3 in analogy to the homogeneous systems (so-called Grubbs-II catalysts, vide infra). Conversely, the observed evidence of interactions of the imidazolium moiety with the silica surface in **Mat-ImF** combined with the absence of Ru coordinated PCy_3 in **Mat-RuF** is consistent with the formation of a NHC−Ru alkylidene species that is most likely stabilized by surface oxygen atoms, and which could be viewed as an equivalent of the so-called Grubbs−Hoveyda-II catalysts.[2] Note that the corresponding molecular complexes, **RuF** and **RuR**, prepared by the same approach (reaction of the imidazolium with $K\{N(SiMe_3)_2\}$ and then $[(Cl)_2Ru(=CHPh)(PCy_3)_2]$), have both one NHC and one PCy_3 ligand (Scheme 1d,e), further indicating the specificity of the surface in **Mat-RuF** having a flexible tether.

We then investigated the catalytic performance of both systems with the rigid and flexible tethers, to ask whether the presence or the absence of metal-surface interactions affects the catalytic performance of supported catalysts. We examined three standard reactions (Table 1) that are sensitive to the structure of the catalysts:

(1) Self-metathesis of ethyl oleate, a pure functionalized Z-dissymmetric alkene, for which the stereochemical outcome of the reaction (E/Z ratio) is a fingerprint of the active sites (each catalyst displays a characteristic E/Z ratio).[4,13]

(2) Tandem ring-opening−ring-closing metathesis (RO-RCM) of cyclooctene. This reaction is very sensitive to the NHC ligand architecture, providing either dimer/trimer or polymers.[10]

(3) Ring-closing metathesis (RCM) of diallyl diethyl malonate, a classical alkene metathesis substrate used to evaluate catalyst activity and stability.[14]

In the metathesis of ethyl oleate, it is noteworthy that **Mat-RuF** rapidly converts ethyl oleate to the expected thermodynamic mixtures (ca. 50% conv.) within 5 h. Under identical conditions **Mat-RuR** deactivates rapidly, leading to only 17% conversion; allowing longer reaction times does not improve conversion. This behavior is in sharp contrast with their homogeneous equivalents as both **RuF** and **RuR** convert ethyl oleate to the thermodynamic equilibrium mixture in less than 5 h. Additionally note that all of the catalysts display similar Z/E ratios (ca. 2) at extrapolated 0% conversion, which indicates that homogeneous and heterogeneous catalysts may have related catalytically active site structures.[10]

In the tandem RO-RCM of cyclooctene, we observed that **Mat-RuF** again displayed much greater catalytic performance than **Mat-RuR**, especially in terms of stability since the latter could only reach 25% conversion (vs 95% conversion for the former). Although **Mat-RuF** and its homogeneous analogue

Table 1. Comparison of Catalytic Performance in Well-Defined Ru−NHC Alkene Metathesis Catalysts

Performance	Catalysts			
	Mat-RuF	Mat-RuR	RuF	RuR
Reaction **1**[a]	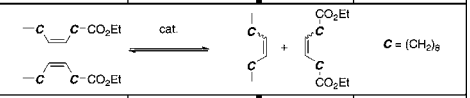			
Conversion @ (time)	47% (5h)	17% (5h)[c]	52% (0.3h)	50% (5h)
Initial rates[d] /h^{-1}	14000	3700	43000	23000
Selectivity[b]	1.8	2.0	2.1	2.0
Reaction **2**[e]	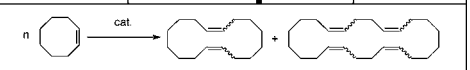			
Conversion @ (time)	95% (24h)	25% (24h)	100% (24h)	100% (24h)
Initial rates /h^{-1}	1360	260	1090	510
Selectivity[f] (Mass balance)	53/22 (90%)	45/20 (80%)	51/23 (90%)	52/25 (87%)
Reaction **3**[g]	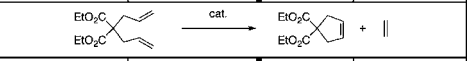			
Conversion @ (time)	57% (3h)	47% (3h)	87% (3h)	94% (3h)
Selectivity[h]	> 95 %	> 95 %	> 95 %	> 95 %

[a]Self-metathesis of neat ethyl oleate (EO) was carried out at 40 °C with EO/Ru = 10 000. [b]Ratio of cis to trans products extrapolated to 0% conversion. [c]No conversion past that time. [d]Initial rates are taken at the most active stage of the catalyst (after the initiation period). [e]The tandem ring-opening−ring-closing metathesis of cyclooctene (cC_8) was carried out at 25 °C in toluene (20 mM cC_8) with cC_8/Ru = 10 000. [f]Selectivity in dimers/trimers. [g]Ring-closing metathesis of diethyl diallyl malonate (DEDAM) was carried out at 50 °C in toluene with DEDAM/Ru = 1000; no rates were measure in that case. [h]As measured by NMR spectroscopy.

RuF both display similar very good performance (ca. 1360 vs 1090 h^{-1} initial rates and 100% conversion), **RuR** clearly outperformed its heterogeneous variant (**Mat-RuR**) in terms of initial rates (510 h^{-1} vs 260 h^{-1}) and stability (100% conversion vs 25% conversion; Table 1). Third, in the RCM of diallyl diethyl malonate, the catalytic performances were similar for the **RuR** and **RuF** family; the only difference resided in that homogeneous catalysts were slightly more stable (ca. 90% conversion) than their heterogeneous analogues (ca. 50% conversion).

The differences in catalytic performance between the two heterogeneous catalysts are fully consistent with the fact that metal-surface interactions have a dramatic effect on the reactivity and stabilization of reactive intermediates,[15] hence the slightly lower activity of the heterogeneous catalysts and the large difference in productivity between **Mat-RuF** and **Mat-RuR**. Considering that for all metathesis catalysts a 14-electron active species must be generated through loss of a coordinating ligand (PCy_3 for **Mat-RuR** and for the homogeneous catalysts vs the surface oxygen functionalities for **Mat-RuF**), the aforementioned observation can be interpreted as follows (Scheme 3). For **Mat-RuR** this step is likely irreversible, in contrast to the homogeneous catalysts, since free PCy_3 reacts

dx.doi.org/10.1021/ja311722k | J. Am. Chem. Soc. 2013, 135, 3193−3199

Scheme 3. Formation of the Active Species and Successive Reactions

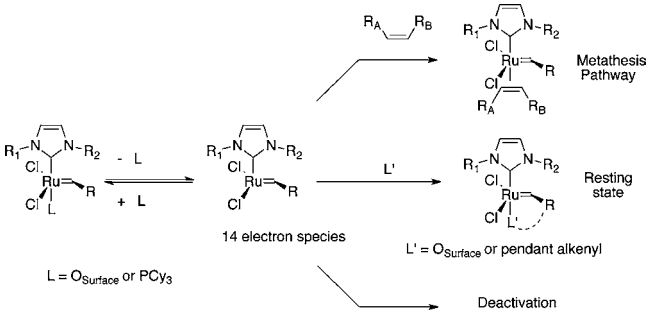

with surface functionalities. After initiation, the propagating alkylidene species in **Mat-RuR** is therefore a free unstable 14-electron reactive species. In the self-metathesis of ethyl oleate, this highly reactive species will either react or decompose very rapidly. In contrast, for **Mat-RuF**, this species can either react with the alkene moiety of ethyl oleate or coordinate back to the oxygen functionalities of the surface, providing a stable resting state for the catalytic active sites. On the other hand, in the RCM of diethyl diallyl malonate, the alkylidene intermediates bear a γ-alkenyl fragment, which can stabilize a 14-electron active species. This would explain why there is hardly any difference between the two heterogeneous catalysts in this specific reaction; both being stabilized by the pendant alkenyl group. However, in tandem RO-RCM, backbiting of the remote pendant alkenyl functionality is probably not as efficient, and surface interactions again become important for the stabilization of unstable 14-electron Ru intermediates, hence the difference in stability of **Mat-RuF** and **Mat-RuR**.

CONCLUSION

In conclusion, our study shows that the performance of the catalytic centers in immobilized Ru−NHC systems is greatly influenced by the nature of the tether, a flexible tether providing higher stability. Experimental evidence suggests that this results from surface interactions, which enable the stabilization of reactive intermediates (as resting states), a phenomenon typically encountered in bio- or homogeneous catalysts where residues and ligands play an essential role. This opens new perspectives in the design of heterogeneous catalysts where interactions with the surface, or even tailored secondary surface functional groups, can be implemented to favor or disfavor a specific reaction pathway.

EXPERIMENTAL SECTION

General Procedure. All organometallic syntheses, passivation steps and grafting experiments for the introduction of the metal complex were carried out under argon using standard Schlenk techniques, using dry and degassed solvents. Toluene was freshly distilled over NaK under Ar in the presence of benzophenone ketyl. Dichloromethane was freshly distilled over P_2O_5. Tetraethoxysilane (TEOS) was distilled over Mg under Ar. Triethylamine, Pluronic P123, tetramethylsilyl bromide (TMSBr), potassium hexamethyldisilazide K{N($SiMe_3$)$_2$} (0.5 M in toluene), and Grubbs I catalyst [$Cl_2(PCy_3)_2Ru(=CHPh)$] were bought from Sigma-Aldrich, and chlorobenzyltriethoxysilane and 3-chloropropyltriethoxysilane were from ABCR. Cyclooctene was purchased from Aldrich, distilled over Na prior to use. Diethyl diallyl malonate (DEDAM) was purchased from Sigma-Aldrich and purified over alumina prior to use. Ethyl oleate was purchased from Nu-Chek Prep and purified over alumina prior to use. Elemental analyses were performed at the microanalysis center in Pascher, Germany. Analysis by gas phase chromatography was performed on a Hewlett-Packard 5890 series II GC apparatus equipped with a FID detector and a Fame column (50 m × 0.25 mm) to monitor the metathesis of ethyl oleate and on an Agilent Technologies 7890A GC apparatus equipped with a FID detector and a HP5 column (30 m × 0.32 mm) for RCM of DEDAM and RO-RCM of cyclooctene. Split ratio of GC was set to 50:1. Sample injection was 1 μL with a 10-μL syringe. Liquid-state NMR spectra were recorded using a Bruker AC 300 and solid-state NMR spectra were recorded under MAS on Bruker Avance 300 and 500 MHz spectrometers with a conventional double resonance 4 mm CP-MAS probe. The MAS frequency was set to 10 kHz for all of the experiments reported here. The samples were introduced in a 4 mm zirconia rotor in the glovebox and tightly closed.

Surface-Enhanced NMR by Dynamic Nuclear Polarization (SENS). All SENS experiments were performed using a solid-state DNP-NMR spectrometer designed by Bruker-Biospin with specifications given by Rosay et al.[16] This system consists of a wide-bore 9.4 T magnet ($\omega_H/(2\pi)$ = 400 MHz, $\omega_{Si}/(2\pi)$ = 79.4 MHz) with a Bruker Avance III spectrometer console, and is equipped with a triple resonance 3.2 mm low-temperature CPMAS probe. DNP is achieved by irradiating the sample with microwaves at a frequency of 263 GHz. The microwaves are generated by a gyrotron and delivered to the sample by a corrugated waveguide with ∼5 W of power reaching the sample. Sapphire rotors (endowed with ZrO_2 caps) were used for optimal microwave penetration. The MAS spinning frequencies were regulated to 8 kHz ± 2 Hz, the sample temperatures were ∼100 K. ^{1}H and ^{29}Si Chemical shifts are referenced to DSS at 0 ppm. The pulse sequence for 2D ^{1}H−^{29}Si HETCOR DNP SENS correlation spectra is shown in Figure S1. The polarization delay (for DNP) between scans was 1.5 s in all experiments. The ^{1}H $\pi/2$ pulse length was 2.8 μs (ν_1 = 89 kHz). A linear amplitude ramp (from 90% to 100% of the nominal RF field strength) was used for the ^{1}H channel, with a 400 μs CP contact time τ_{CP} and a nominal RF field amplitude (ν_1) of 64 kHz for ^{1}H and 60 kHz for ^{29}Si. SPINAL-64[17] proton decoupling was applied during the acquisition of the ^{29}Si signal with ν_1 = 89 kHz. The eDUMBO-1_{22} scheme[18] was used for ^{1}H homonuclear decoupling during the indirect evolution time with ν_1 = 89 kHz (and a basic eDUMBO cycle of 34 μs). A scaling factor of 0.56 was applied to correct the ^{1}H chemical shift scale.[18] Quadrature detection was achieved using the States-TPPI[19] scheme by incrementing the phase of the ^{1}H spin-lock pulse of the CP step. A total of 128 t_1 increments of 64 μs each were recorded, the overall acquisition times in t_1 and t_2 were 4.3 and 11.4 ms, respectively. The spectra in Figure 1A,B (main text) were recorded with 16 and 128 scans per increment, respectively. The 2D spectra were processed with a 2048 × 1024 complex points, and 80 Hz of exponential line broadening was applied in both dimensions prior to Fourier transformation. Proton DNP enhancement factors (ϵ_H) were determined by scaling the intensities of the direct excitation ^{1}H spectra obtained under the same experimental conditions with or without MW irradiation.

Preparation of Homogeneous Catalysts.

*Synthesis of **RuF**.* **RuF** was prepared according to the reported procedure.[4]

*Synthesis of **RuR**.* To the solution of 4-{4′-(tri(isopropoxy)silyl)-phenyl}-2,6-dimethylphenyl imidazole (0.63 g, 1.41 mmol) in toluene (10 mL) was added benzyl chloride (0.18 g, 1.41 mmol). After heating the reaction mixture for 24 h under reflux, the solid was filtered, washed with pentane (2 × 20 mL), and dried under vacuum to yield 1-{4′-[4″-(tri(isopropoxy)silylphenyl]-2′,6′-dimethylphenyl}-3-benzyl-imidazolium chloride as a white solid (**ImR**). ^{1}H NMR (CD_2Cl_2, 300 MHz): δ (ppm) = 11.25 (s, 1H). 7.77 (d, $^3J_{HH}$ = 8 Hz, 2H), 7.62−7.60 (m, 5H), 7.51−7.44 (m, 7H), 7.43 (s, 1H, NC*H*CHN), 7.21 (s, 1H, NCHC*H*N), 5.95 (s, 2H, CH_2), 4.30 (sept, 3H, $^3J_{HH}$ = 6 Hz C*H*(CH_3)$_2$), 2.21 (s, 6H, o-CH_3), 1.23 (d, $^3J_{HH}$ = 6 Hz, 18H, (−CH(*C*H_3)$_2$)$_3$. ^{13}C NMR (CD_2Cl_2, 75 MHz): δ (ppm) = 143.7, 140.7, 139.3, 135.4, 135.2, 133.8, 129.4, 129.3, 129.0, 127.9, 126.4, 123.1, 122.1, 65.5 (-*C*H(CH_3)$_2$), 25.3 (−CH(*C*H_3)$_2$), 17.8 (Ar−CH_3). HRMS (ESI+): m/z 543.3026 [M−Cl]$^+$, i.e., calculated 543.3037. To a mixture of **ImR** (0.35 g, 0.60 mmol) in 5 mL of toluene, was added

dx.doi.org/10.1021/ja311722k | J. Am. Chem. Soc. 2013, 135, 3193−3199

1.45 mL (0.72 mmol) of a 0.5 M toluene solution of K{N(SiMe$_3$)$_2$}. After stirring the reaction mixture for 20 min, [Cl$_2$(PCy$_3$)$_2$Ru(=CHPh)] (0.44 g, 0.54 mmol) in 10 mL of toluene was added. The reaction mixture was stirred for 3 h and filtered over Celite. After removal of the solvent under vacuum the residual solid was crystallized in toluene and pentane yielding 0.16 g of **RuR** (42%). ^{1}H NMR (CD_2Cl_2, 300 MHz): δ (ppm) = 19.24 (s, 1H), 7.93 (br, 1H), 7.76−7.49 (m, 5H), 7.39 (t, 1H, J = 7.5 Hz), 7.25−6.98 (m, 5H), 6.88 (br, 2H), 5.92 (s, 2H), 4.32 (m, 1H, -C$\underline{H}$(CH$_3$)$_2$) 2.30 (m, 4H), 2.10 (s, 6H), 1.64−1.53 (m, 18H), 1.24 (d, 18H, J = 6 Hz) 1.22−1.07 (m, 14H). ^{31}P NMR (CD_2Cl_2, 125 MHz): δ (ppm) = 36.4 (s, 1P). ^{13}C NMR (CD_2Cl_2, 75 MHz): δ (ppm) = 294.4 (HC=Ru), 187.7 (C_{NHC}-Ru, J_{P-C} = 75 Hz), 151.8, 141.9, 141.3, 138.5, 137.3, 135.7, 135.4, 132.2, 130.3, 129.8, 129.3, 129.0, 128.6, 126.7, 124.3, 121.5, 65.9 (-$\underline{C}$H(CH$_3$)$_2$), 55.5 (-NCH$_2$Ph), 31.8 (d, J_{P-C} = 16.5 Hz, *ipso*-C$_{Cy}$), 29.9 (*meta*-C$_{Cy}$), 28.1 (d, J_{P-C} = 9.8 Hz *ortho*-C$_{Cy}$), 26.9 (*para*-C$_{Cy}$), 25.7 (−CH($\underline{C}$H$_3$)$_2$), 18.7 (Ar−CH$_3$). HRMS (ESI+): m/z 1049.4478 [M−Cl]$^+$, i.e., calculated 1049.4493.

Preparation of Heterogeneous Catalysts.

*Synthesis of **Mat-RuF**.* **Mat-RuF** was synthesized according to literature procedure.[4]

*Synthesis of **Mat-RuR**.* A mixture of 2.70 g of P123 dissolved in an aqueous HCl solution (109 mL, pH 1.5) was added to a mixture of TEOS (6.07 g, 29.2 mmol) and 4-{4′-(tri(isopropoxy)silyl)phenyl}-2,6-dimethylphenylimidazole (0.44 g, 0.97 mmol) at room temperature. The reaction mixture was stirred for 90 min giving rise to a microemulsion (transparent mixture). To the reaction mixture heated at 45 °C was added small amount of NaF (15 mg) under stirring (mixture composition: 0.04 F-/1 TEOS/0.033 of 4-{4′-(tri-(isopropoxy)silyl)phenyl}-2,6-dimethylphenylimidazole/0.016 P123/0.12 HCl/220 H$_2$O). The mixture was left at 45 °C under stirring for 72 h. The resulting solid was filtered and washed with acetone. The surfactant was removed by an extraction with ethanol using a Soxhlet during 24 h. After filtration and drying at 135 °C under vacuum 2.95 g of **Mat-R** was obtained. Elemental analysis: N = 1.02%$_{wt}$, Si = 40.0%$_{wt}$. Si/N ratio obtained: 19 (expected 20). To **Mat-R** (0.8 g) was added toluene (15 mL) and benzyl chloride (0.62 mL, 15 equiv). After heating the reaction mixture at 135 °C for 72h, the solid was recovered by filtration and washed successively with toluene (3 × 100 mL), acetone (3 × 100 mL) and diethyl ether (3 × 50 mL). The solid was then dried for 14 h under high vacuum (10^{-5} mbar) at 135 °C, affording 0.75 g of nonhydrolyzed material. To this material (0.7 g) was added 5 mL of a 2 M aqueous HCl. After heating the reaction mixture at 45 °C for 2 h under stirring, the solid was filtered and washed successively with water (3 × 100 mL), acetone (3 × 100 mL) and diethyl ether (3 × 50 mL). The solid was then dried for 5−6 h under high vacuum (10^{-5} mbar) at 135 °C, to afford 0.6 g of hydrolyzed material. To this material (0.55 g) was added a mixture of pyridine (4.1 mL), water (4.1 mL), and 2 M aqueous HCl (0.7 mL).[5a] After heating the reaction mixture at 70 °C for 22 h, the solid was filtered and washed successively with water (3 × 100 mL), acetone (3 × 100 mL), and diethyl ether (3 × 100 mL). The solid was then dried for 14 h under high vacuum (10^{-5} mbar) at 135 °C, affording 0.5 g of **Mat-ImR**. ^{1}H solid-state NMR (500 MHz): 7.6 ppm (aromatic H), 2.1 (Me$_2$C$_6$H$_2$). ^{13}C CP-MAS solid-state NMR (125 MHz): 134−127 ppm (Car) 54 ppm (NCH$_2$Ph), 15 ppm (Me$_2$C$_6$H$_2$). To the suspension of **Mat-ImR** (0.4 g) in toluene (28.0 mL) was added triethylamine (5.1 mL) and TMSBr (2.5 mL) at room temperature. The reaction mixture was stirred overnight. The solid was further filtered and washed successively with toluene (3 × 20 mL) and dichloromethane (3 × 20 mL). The solid was dried under high vacuum (10^{-5} mbar) for 16 h at 135 °C, affording 0.4 g of passivated **Mat-ImR**. To the suspension of passivated **Mat-ImR** (0.38 g, 1.0 equiv) in toluene (2.0 mL) was slowly added a 0.5 M toluene solution of K{N(SiMe$_3$)$_2$} (0.4 mL, 1.2 equiv) at room temperature. After stirring for 30 min, [Cl$_2$(PCy$_3$)$_2$Ru(=CHPh)] (0.16 g, 1.2 equiv) in toluene (4.0 mL) was slowly added at room temperature to the reaction mixture. After stirring the reaction mixture for 20 h, the solid was filtered and washed successively with toluene (2 × 20 mL) and dichloromethane (3 × 20 mL) till the filtrate was colorless. The material was dried under high vacuum (10^{-5} mbar) at room temperature for 22 h to yield 0.35 g of a light greenish **Mat-RuR**. ^{1}H solid-state NMR (300 MHz): δ (ppm) = 7.3 (aromatic H), 0.0 (Me$_3$Si). ^{13}C CP-MAS solid-state NMR (75 MHz): δ (ppm) = 134−128 (aromatic C), 54 (NCH$_2$Ph), 26 (PCy$_3$), 17 (Me$_2$C$_6$H$_2$), 0 (Me$_3$Si). ^{29}Si CP-MAS solid-state NMR: δ (ppm) = +11.9 (OSiMe$_3$), −82.3 (T$_3$), −101.5 (Q$_3$), −109.6 (Q$_4$). ^{31}P solid-state NMR (75 MHz): δ (ppm) = 50 (P(V)), 37 (Ru-PCy$_3$). Elemental analysis: N = 1.13%$_{wt}$; Ru = 1.40%$_{wt}$, P = 0.40%$_{wt}$. N/Ru ratio obtained: 0.17 (expected 0.5).

Representative Procedure for Metathesis Reactions.

Self-Metathesis of Ethyl Oleate. General Procedure. All metathesis experiments were carried out under an inert atmosphere of argon. In a typical run, a 5 mL Schlenk flask was loaded with ethyl oleate and Ru-catalysts [**Mat-RuR**, **Mat-RuF**, **Ru-R**, and **Ru-F**] in a 10000:1 ratio, and the reaction mixture was heated at 40 °C. After certain interval of time an aliquot of the reaction mixture was drawn, quenched with ethyl acetate, and analyzed by GC.

Ring-Opening−Ring-Closing Metathesis (RO-RCM) of cis-Cyclooctene. The reaction was carried out as described above using a ∼20 mM solution of cyclooctene in toluene with 0.01% of Ru catalysts, a reaction temperature of 25 °C, and eicosane as internal standard.

Ring-Closing Metathesis (RCM) of DEDAM. The reaction was carried out as described above using a ∼20 mM solution of DEDAM with 0.1% of Ru catalysts, a reaction temperature of 50 °C, and eicosane as internal standard.

■ ASSOCIATED CONTENT

Ⓢ Supporting Information

Synthesis scheme for molecular catalyst **Ru-R**, pulse sequences for DNP, additional characterization spectra of products, and catalytic test. This material is available free of charge via the Internet at http://pubs.acs.org.

■ AUTHOR INFORMATION

Corresponding Author

ccoperet@ethz.ch; thieuleux@cpe.fr

Notes

The authors declare no competing financial interest.

■ ACKNOWLEDGMENTS

This work was supported in part by the "Agence Nationale de la Recherche" (ANR-08-BLAN-0151). Financial support is acknowledged from EQUIPEX Contract No. ANR-10-EQPX-47-01 and ETH Zürich. The authors wish to thank Drs. Werner Maas, Shane Pawsey, and Melanie Rosay and Bruker Biospin Corporation (Billerica, U.S.A.) for support with the DNP-SSNMR spectrometer.

■ REFERENCES

(1) (a) Grubbs, R. H. *Angew. Chem., Int. Ed.* **2006**, *45*, 3760−3765. (b) Vougioukalakis, G. C.; Grubbs, R. H. *Chem. Rev.* **2010**, *110*, 1746−1787.

(2) (a) Herrmann, W. A. *Angew. Chem. Int. Ed.* **2002**, *41*, 1290−1309. (b) Deshmukh, P. H.; Blechert, S. *Dalton Trans.* **2007**, 2479−2491. (c) Monfette, S.; Fogg, D. E. *Chem. Rev.* **2009**, *109*, 3783−3816. (d) Samojlowicz, C.; Bienek, M.; Grela, K. *Chem. Rev.* **2009**, *109*, 3708−3748. (e) Hoveyda, A. H.; Malcolmson, S. J.; Meek, S. J.; Zhugralin, A. R. *Angew. Chem., Int. Ed.* **2010**, *49*, 34−44. (f) Nolan, S. P.; Clavier, H. *Chem. Soc. Rev.* **2010**, *39*, 3305−3316.

(3) For reviews, see: (a) Buchmeiser, M. R. *New J. Chem.* **2004**, *28*, 549−557. (b) Copéret, C.; Basset, J. M. *Adv. Synth. Catal.* **2007**, *349*, 78−92. (c) Clavier, H.; Grela, K.; Kirschning, A.; Mauduit, M.; Nolan, S. P. *Angew. Chem., Int. Ed.* **2007**, *46*, 6786−6801. (d) Buchmeiser, M. H. *Chem. Rev.* **2009**, *109*, 303−321. For seminal and selected reports in the field: (e) Mayr, M.; Mayr, B.; Buchmeiser, M. R. *Angew. Chem.,*

Int. Ed. **2001**, *40*, 3839−3842. (f) Pruehs, S.; Lehmann, C. W.; Fuerstner, A. *Organometallics* **2004**, *23*, 280−287. (g) Halbach, T. S.; Mix, S.; Fischer, D.; Maechling, S.; Krause, J. O.; Sievers, C.; Blechert, S.; Nuyken, O.; Buchmeiser, M. R. *J. Org. Chem.* **2005**, *70*, 4687−4694. (h) Allen, D. P.; vanWingerden, M. M.; Grubbs, R. H *Org. Lett.* **2009**, *11*, 1261−1264.

(4) Karame, I.; Boualleg, M.; Camus, J. M.; Maishal, T. K.; Alauzun, J.; Basset, J. M.; Copéret, C.; Corriu, R. J. P.; Jeanneau, E.; Mehdi, A.; Réyé, C.; Veyre, L.; Thieuleux, C. *Chem.—Eur. J.* **2009**, *15*, 11820−11823.

(5) (a) Mehdi, A.; Reye, C.; Corriu, R. J. P. *Chem. Soc. Rev.* **2011**, *40*, 563−574. (b) Hoffmann, F.; Cornelius, M.; Morell, J.; Froba, M. *Angew. Chem., Int. Ed.* **2006**, *45*, 3216−3251.

(6) (a) Copéret, C.; Chabanas, M.; Petroff Saint-Arroman, R.; Basset, J. M. *Angew. Chem., Int. Ed.* **2003**, *42*, 156−181. (b) Thomas, J. M.; Raja, R.; Lewis, D. W. *Angew. Chem., Int. Ed.* **2005**, *44*, 6456−6482. (c) Tada, M.; Iwasawa, Y. *Coord. Chem. Rev.* **2007**, *251*, 2702−2716. (d) Wegener, S. L.; Marks, T. J.; Stair, P. C. *Acc. Chem. Res.* **2012**, *45*, 206−214.

(7) Maishal, T. K.; Alauzun, J.; Basset, J.-M.; Copéret, C.; Corriu, R. J. P.; Jeanneau, E.; Mehdi, A.; Reye, C.; Veyre, L.; Thieuleux, C. *Angew. Chem., Int. Ed.* **2008**, *47*, 8654−8656.

(8) (a) Lesage, A.; Lelli, M.; Gajan, D.; Caporini, M. A.; Vitzthum, V.; Mieville, P.; Alauzun, J.; Roussey, A.; Thieuleux, C.; Mehdi, A.; Bodenhausen, G.; Copéret, C.; Emsley, L. *J. Am. Chem. Soc.* **2010**, *132*, 15459−15461. (b) Lelli, M.; Gajan, D.; Lesage, A.; Caporini, M. A.; Vitzthum, V.; Mieville, P.; Heroguel, F.; Rascon, F.; Roussey, A.; Thieuleux, C.; Boualleg, M.; Veyre, L.; Bodenhausen, G.; Copéret, C.; Emsley, L. *J. Am. Chem. Soc.* **2011**, *133*, 2104−2107. (c) Rossini, A. J.; Zagdoun, A.; Lelli, M.; Gajan, D.; Rascon, F.; Rosay, M.; Maas, W. E.; Copéret, C.; Lesage, A.; Emsley, L. *Chem. Sci.* **2012**, *3*, 108−115. (d) Zagdoun, A.; Casano, G.; Ouari, O.; Lapadula, G.; Rossini, A. J.; Lelli, M.; Baffert, M.; Gajan, D.; Veyre, L.; Maas, W. E.; Rosay, M.; Weber, R. T.; Thieuleux, C.; Copéret, C.; Lesage, A.; Tordo, P.; Emsley, L. *J. Am. Chem. Soc.* **2012**, *134*, 2284−2291. (e) Zagdoun, A.; Rossini, A. J.; Gajan, D.; Bourdolle, A.; Ouari, O.; Rosay, M.; Maas, W. E.; Tordo, P.; Lelli, M.; Emsley, L.; Lesage, A.; Copéret, C. *Chem. Commun.* **2012**, *48*, 654−656. (f) Rossini, A. J.; Zagdoun, A.; Lelli, M.; Canivet, J.; Aguado, S.; Ouari, O.; Tordo, P.; Rosay, M.; Maas, W. E.; Copéret, C.; Farrusseng, D.; Emsley, L.; Lesage, A. *Angew. Chem., Int. Ed.* **2012**, *51*, 123−127. (g) Vitzthum, V.; Mieville, P.; Carnevale, D.; Caporini, M. A.; Gajan, D.; Copéret, C.; Lelli, M.; Zagdoun, A.; Rossini, A. J.; Lesage, A.; Emsley, L.; Bodenhausen, G. *Chem. Commun.* **2012**, *48*, 1988−1990.

(9) Song, C. S.; Hu, K. N.; Joo, C. G.; Swager, T. M.; Griffin, R. G. *J. Am. Chem. Soc.* **2006**, *128*, 11385−11390.

(10) Kavitake, S.; Samantaray, M. K.; Dehn, R.; Deuerlein, S.; Limbach, M.; Schachner, J. A.; Jeanneau, E.; Copéret, C.; Thieuleux, C. *Dalton Trans.* **2011**, *40*, 12443−12446.

(11) (a) Sommer, J.; Yang, Y.; Rambow, D.; Bluemel, J. *Inorg. Chem.* **2004**, *43*, 7561−7563. (b) Hilliard, C. R.; Bhuvanesh, N.; Gladysz, J. A.; Bluemel, J. *Dalton Trans.* **2012**, *41*, 1742−1754.

(12) Chabanas, M.; Baudouin, A.; Copéret, C.; Basset, J. M.; Lukens, W.; Lesage, A.; Hediger, S.; Emsley, L. *J. Am. Chem. Soc.* **2003**, *125*, 492−504.

(13) Copéret, C. *Beilstein J. Org. Chem.* **2011**, *7*, 13−21.

(14) Ritter, T.; Hejl, A.; Wenzel, A. G.; Funk, T. W.; Grubbs, R. H. *Organometallics* **2006**, *25*, 5740−5745.

(15) (a) Blanc, F.; Copéret, C.; Thivolle-Cazat, J.; Basset, J.-M.; Lesage, A.; Emsley, L.; Sinha, A.; Schrock, R. R. *Angew. Chem., Int. Ed.* **2006**, *45*, 1216−1220. (b) Copéret, C. *Pure Appl. Chem.* **2009**, *81*, 585−596.

(16) Rosay, M.; Tometich, L.; Pawsey, S.; Bader, R.; Schauwecker, R.; Blank, M.; Borchard, P. M.; Cauffman, S. R.; Felch, K. L.; Weber, R. T.; Temkin, R. J.; Griffin, R. G.; Maas, W. E. *Phys. Chem. Chem. Phys.* **2010**, *12*, 5850−5860.

(17) Elena, B.; de Paepe, G.; Emsley, L. *Chem. Phys. Lett.* **2004**, *398*, 532−538.

(18) Fung, B. M.; Khitrin, A. K.; Ermolaev, K. *J. Magn. Reson.* **2000**, *142*, 97−101.

(19) Marion, D.; Ikura, M.; Tschudin, R.; Bax, A. *J. Magn. Reson.* **1989**, *85*, 393−399.